ELSEVIER

Catalysis Today 48 (1999) 139–145

CATALYSIS TODAY

A homogeneous-heterogeneously catalysed reaction system in a loop reactor

T. Salmi[a,*], J. Lehtonen[a], J. Kaplin[a], A. Vuori[b], E. Tirronen[b], H. Haario[c]

[a]*Laboratory of Industrial Chemistry, Åbo Akademi, Turku, Finland*
[b]*Kemira Research Centre, Espoo, Finland*
[c]*Profmath Oy, Helsinki, Finland*

Abstract

Catalytic three-phase reactions including homogeneous liquid-phase steps were simulated in a loop reactor. The loop reactor consisted of a reaction vessel, an external loop as well as an ejector. The loop reactor was modelled using tanks-in-series or alternatively, axial dispersion models. Kinetics of the reductive alkylation of aromatic amines, which was determined from the experiments in a laboratory autoclave, was used for verifying the reactor model and for concentration profile simulations in the loop reactor.

Keywords: Loop reactor; Catalytic and non-catalytic reactions; Reductive alkylation of amines

1. Introduction

Loop reactors equipped with external recycling and heat exchangers are particularly suitable for gas–liquid reactions and catalytic three-phase reactions. The reactor construction is simple and the gas–liquid contact is efficient. The present work concerns generalized modelling of a catalytic loop reactor. A homogeneous-heterogeneously catalysed chemical system, reductive alkylation of aromatic amines, was used as a demonstration system.

A principal sketch of the loop reactor is presented in Fig. 1. The building blocks of the system are the reaction vessel, the external loop and the ejector. The size of the reaction vessel of the particular loop reactor was 7 m^3 and the length of the loop was about 10 m with volume 1 m^3. The reacting gas, e.g. hydrogen, is mixed with the liquid phase in the ejector and the cocurrent gas–liquid flow is pumped into the reactor. The liquid phase is recirculated through an external heat exchanger back to the ejector. Since one liquid reactant is fed to the upper part of the reaction vessel and the hydrogen pressure is maintained constant, the reactor is operated dynamically.

2. Loop reactor modelling

Several approaches are in principle possible in the quantitative description of the loop reactor. However, in the present work, the main focus was put on the chemical process; thus we remained at a hydrodynamically simplified approach. The building blocks of the system were modelled separately: the reactor itself was described with two stirred tanks-in-series, the

*Corresponding author. Tel.: +358-2-2154427; fax: +358-2-2154479.

0920-5861/99/$ – see front matter
PII: S0920-5861(98)00368-X

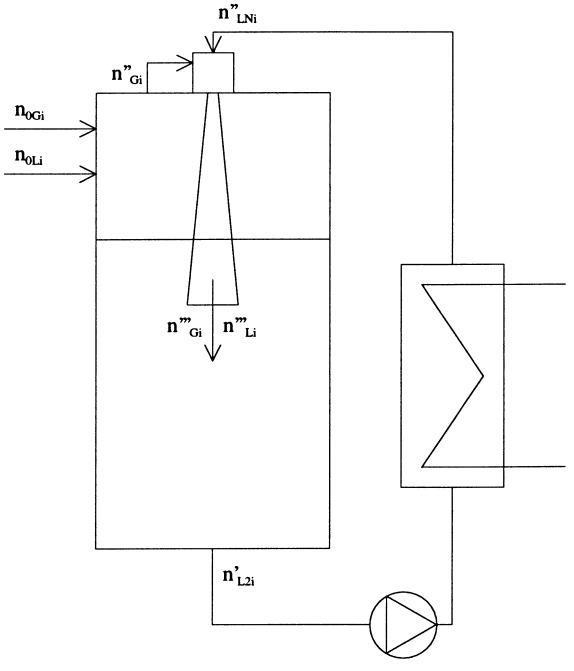

Fig. 1. A principal sketch of the loop reactor.

loop was treated as dynamic CSTRs coupled in series or alternatively with a dynamic axial dispersion model. The ejector was simply considered as a mixing unit with a negligible reaction volume. Because of the vigorous mixing and very minor temperature difference between the reactor and the loop, an isothermal model was considered to be sufficient. The gas–liquid mass-transfer effects were included in the model, whereas the intraparticular mass-transfer resistance was ignored because of finely dispersed catalyst particles. The reactor model equations are summarized below.

The model for the reaction vessel (cascade of two CSTRs):

CSTR 1 (liquid phase):

$$\frac{dn'_{L1i}}{dt} = r'_{1i,noncat}V'_{L1} + r'_{1i,cat}m'_{cat,1}c_M + N'_{L1i}A'_1 + \dot{n}_{0Li} + \dot{n}'''_{Li} - \dot{n}'_{L1i}. \quad (1)$$

CSTR 2 (liquid phase):

$$\frac{dn'_{L2i}}{dt} = r'_{2i,noncat}V'_{L2} + r_{2i,cat}m'_{cat,2}c_M + N'_{L2i}A'_2 + \dot{n}'_{L1i} - \dot{n}'_{L2i}. \quad (2)$$

Gas phase:

$$\frac{dn'_{G,H_2}}{dt} = -c_{H_2}\dot{V}_0. \quad (3)$$

The loop models (tanks-in-series model and axial dispersion model)

Tanks-in-series:

$$\frac{dn''_{Lki}}{dt} = r''_{ki,noncat}V''_k + r_{ki,cat}m''_{cat,k}c_M + \dot{n}''_{Lki} - \dot{n}''_{L(k-1)i}. \quad (4a)$$

Axial dispersion:

$$\frac{dn''_{Lki}}{dt} = r''_{ki,noncat}V''_k + r_{ki,cat}m''_{cat,k}c_M - \left(w_L\frac{dc''_{Lki}}{dl} + D_L\frac{d^2c''_{Lki}}{dl^2}\right)V''_k. \quad (4b)$$

The symbols are explained in Section 10.

A general purpose software was developed for the simulation of dynamic semibatch loop reactors. The CSTR-based model, the ordinary differential Eqs. (1)–(4a), were solved with the backward difference method which is suitable for stiff differential equations [1].

The model with axial dispersion in the loop, i.e. the coupled system of ordinary differential equations and partial differential equations (PDEs) (Eq. (4b)) was converted to a system of ODEs by discretizing the PDEs (the loop equations) with respect to the length coordinate. For the first derivatives of the spatial coordinate (the plug flow term in Eq. (4a)), a five-point upwind difference formula was used [2]: whereas the second derivatives describing the axial dispersion were discretized with a five-point central difference formula [2].

The ODE system was solved with the software ODESSA, which includes the stiff ODE solution algorithm (the backward difference method). The ODE solver was a part of a simulation and parameter estimation framework MODEST [3].

3. Gas–liquid mass transfer

Loop reactors are applied on the hydrogenation reactions in order to improve the efficiency of the gas–liquid mass transfer and to diminish the reaction time [4]. The effectiveness of the mass transfer is

focused in the ejector, where the gas is dispersed in the liquid flowing through the ejector throat. The gas–liquid mass transfer in the reaction vessel is ineffective compared to the ejector. It can also be assumed that there is no gas phase present in the loop – all hydrogen is dissoved in the liquid. In our simulation package the mass transfer is described using the simple two-film theory and mass-transfer coefficients based on the effective molecular diffusivities. The hydrogen flux through the gas–liquid interface can be written as follows:

$$N_{L,H_2}a = k_{L,H_2}a(c_{GH_2}/K'_{H_2} - c_{LH_2}), \quad (5)$$

i.e. the mass-transfer rate is assumed to be completely dependent on the liquid-side mass-transfer resistance. In our simulation program, the values of the liquid film mass-transfer coefficients can be estimated according to correlation equations developed for the ejector and the reaction vessel. Experimentally determined values can also be assigned for the coefficients, or the coefficients can be estimated numerically. According to Dirix and van der Wiele [4] the lump of the liquid film mass-transfer coefficient and specific mass-transfer area (k_La) for the ejector is expressed as follows:

$$k_La = \alpha Re_n^2 = \frac{G}{G+L}\frac{D}{V_{ej}^{2/3}}, \quad (6)$$

where Re_n denotes the Reynolds number of the liquid flow at the nozzle of the ejector, D is the diffusion coefficient and V_{ej} denotes the ejector volume. G and L are gas and liquid volumetric flows, respectively; α is an experimental coefficient. In the equation above, it is assumed that the ejector is operating in the bubble flow regime, i.e. $G/L<1.3$. When the bubble flow prevails, the gas–liquid mass transfer in the reactor is negligible [4]. The diffusion coefficient in Eq. (6) is calculated applying the equation of Wilke and Chang [5] for molecular diffusion in mixtures of liquids.

The calculation of the gas–liquid equilibrium ratio for hydrogen ($K' = c_{GH_2}/c_{LH_2}$) is based on the hydrogen solubility in different solvents, e.g. in methanol [6],

$$\ln x_{Li}^{s} = -7.3644 - 408.38/(T/K) \quad (7)$$

and Henry's law. The vapour pressure of the solvent was calculated using Raoult's law and Antoine's equation in order to define the gas-phase composition.

4. Case study: reductive alkylation of amines

The reductive alkylation of aromatic amines is a widely used process in the production of intermediates for the dye-stuff industry. The process is based on the reaction of an aromatic amino group, which reacts with an aldehyde forming a Shiff's base (homogeneous liquid-phase reaction) [7]. The double bond of Shiff's base is then hydrogenated with H_2 [8]. For primary amines, an analogous reaction sequence is

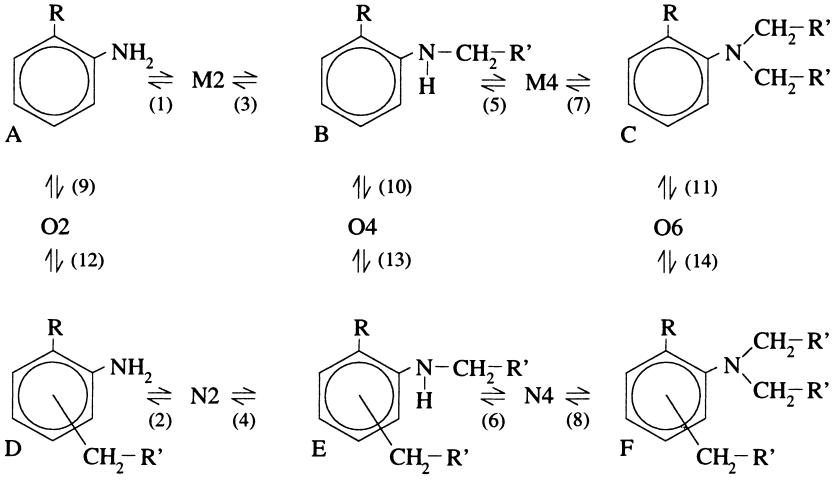

Fig. 2. The reaction scheme of reductive alkylation.

possible for the second hydrogen atom of the amino group, leading to a dialkylated product. Furthermore, dimerization and alkylation of the aromatic ring can appear as side reactions. The complete reaction scheme is shown in Fig. 2.

5. Rate equations

The rate equations of the formation of Shiff's base and its hydrogenation are based on the theories of organic chemical reaction mechanisms. For the homogeneous process, a two-step mechanism was applied, leading to the rate equation

$$R_1 = k_1(c_A c_{R'CHO} - c_{12}c_{H_2O}/K_1K_2). \quad (8)$$

For the hydrogenation step, a Langmuir–Hinshelwood rate equation was used, based on the assumption that the surface reaction between Shiff's base and dissociatively adsorbed hydrogen is the rate determining step. The rate equation of hydrogenation is given below:

$$R_3 = \frac{k_3' c_{12} c_{H_2}}{\left(1 + K_{12}c_{12} + \sqrt{K_H c_{H_2}} + \sum K_j c_j\right)^3}. \quad (9)$$

Based on the reaction stoichiometry, the generation rates of the compounds can be written as follows:

$$r_A = -R_1 - R_9, \quad (10)$$

$$r_B = -R_5 - R_{10} + R_3\rho_B c_M, \quad (11)$$

$$r_C = -R_{11} + R_7\rho_B c_M, \quad (12)$$

$$r_D = -R_2 + R_{12}\rho_B c_M, \quad (13)$$

$$r_E = -R_6 + (R_4 + R_{13})\rho_B c_M, \quad (14)$$

$$r_F = (R_8 + R_{14})\rho_B c_M, \quad (15)$$

$$r_{M2} = R_1 - R_3\rho_B c_M, \quad (16)$$

$$r_{M4} = R_5 - R_7\rho_B c_M, \quad (17)$$

$$r_{N2} = R_2 - R_4\rho_B c_M, \quad (18)$$

$$r_{N4} = R_6 - R_8\rho_B c_M, \quad (19)$$

$$r_{O2} = R_9 - R_{12}\rho_B c_M, \quad (20)$$

$$r_{O4} = R_{10} - R_{13}\rho_B c_M, \quad (21)$$

$$r_{O6} = R_{11} - R_{14}\rho_B c_M. \quad (22)$$

In order to simplify the system for large scale simulation purposes, we choose such a reactant (substituent attached to the aromatic ring and aldehyde chain length) that only mono- and dialkylation reactions were present (reactions 1, 3, 5 and 7).

6. Experimental procedure

The laboratory experiments were carried out in a semibatch-wise operating laboratory autoclave with a volume of 2000 ml. The autoclave was made of steel and equipped with a turbine impeller and a temperature control system. The aromatic reactant dissolved in methanol and the catalyst were placed in the autoclave prior to the experiment, whereas the aldehyde was fed into the reactor during the experiment. Carbon supported Pt with particle sizes of 6–70 μm (80%) was used as a catalyst. The amount of the catalyst was varied from 1 to 3 g catalyst/mol aromatic amine reagent and the content of the active metal in the catalyst ranged from 3 to 5 wt%. The temperature interval of the experiments was 30–75°C and the hydrogen pressure was maintained at 15 bar. The aromatic compounds were analysed with high performance liquid chromatography (HPLC); whereas gas chromatographic (GC) analysis was used for the aldehydes.

7. Parameter estimation

The estimation of kinetic parameters was based on the experimental data obtained for aromatic amines with one alkyl substituent in the ortho position and for the mono- and dialkyted products of this amine. Typical examples of the experimets are displayed in Fig. 3(a) and (b). The rate parameters were estimated by using the rate equations presented above and a dynamic semibatch reactor model describing the laboratory autoclave. The model equations were solved with the backward difference method during the course of parameter estimation, which was carried out with a hybrid Simplex-Marquardt algorithm [9,10] implemented in the sofware MODEST [3]. The fit of the model is illustrated in Fig. 3(a) and (b) and the values of kinetic parameters are given in Table 1. As can be seen from the figures, the model is sufficiently detailed for the description of the reductive alkylation process.

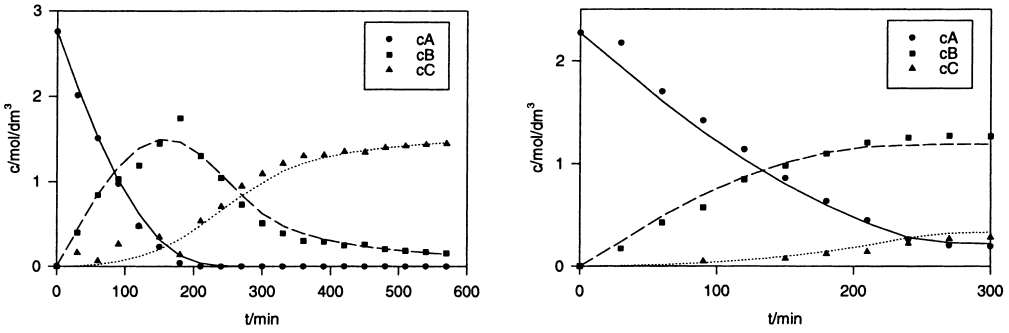

Fig. 3. Two fits of the kinetics model. System: reductive alkylation of an aromatic amine with an aldehyde (number of C-atoms<3).

Table 1
Kinetic parameters of reductive alkylation

R^2=97.66	A (dm^3/(mol min))	σ (%)	E_a (J/mol)	σ (%)
k_1	0.119	9.3	87.3	215
k_5	0.0306	10.7	22690	11.0
	A ((dm^3)^2/(g act. met.) mol min)	σ (%)	E_a (J/mol)	σ (%)
k_3	85.43	109	488.2	214
k_7	5.4E16	0.0	651700	181
	K_{ADS} (dm^3/mol)			
K_{AR}	2.54E−10	157		
K_{H_2O}	5.49E−04	183		
K_{H_2}	1.21E−03	259		
K_{MeOH}	4.34E−03	194		

8. Loop reactor simulations

The loop reactor was simulated using the kinetic model for the reductive alkylation of the aromation amines. In order to verify the model agreement, experiments were carried out in an industrial scale loop reactor. A comparison between the experimental data and the model prediction is presented in Fig. 4. As can be seen from the figure, the model is able to predict the main trends of the reactions in the loop reactor, which is very satisfactory, since the gas–liquid mass transfer in the reactor is a complex phenomenon. In the simulation, Eq. (6) was applied for the calculation of the k_La-value. The coefficient α in Eq. (6) obtains the value 1.58×10^{-3} for the present system.

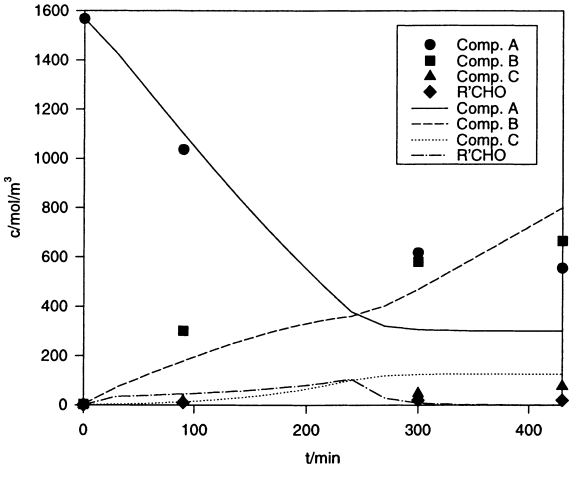

Fig. 4. Model verification in the loop reactor.

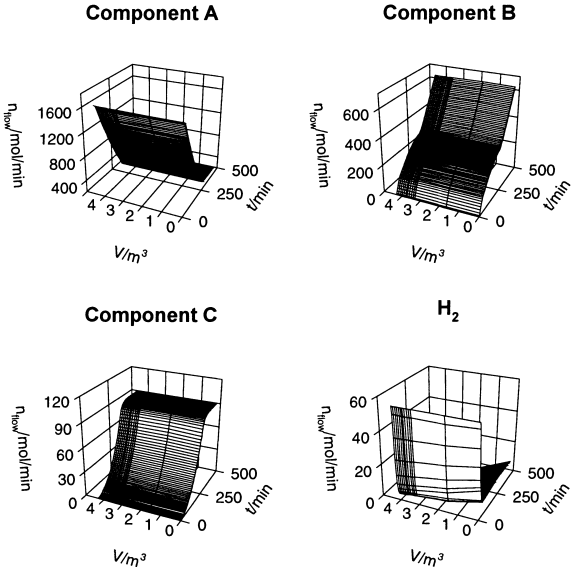

Fig. 5. Profile simulation 1.

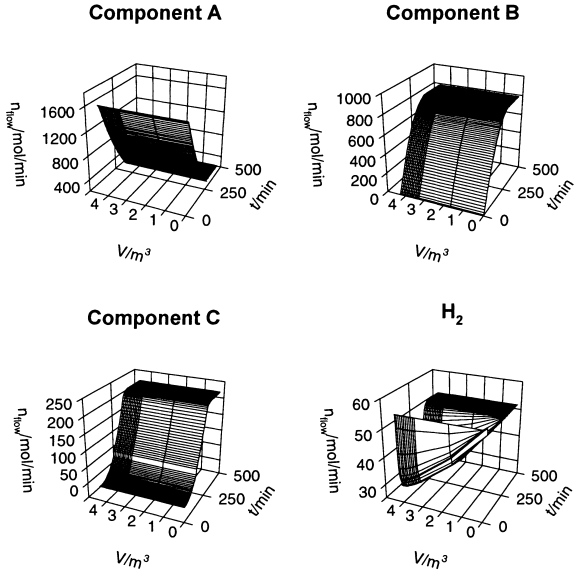

Fig. 6. Profile simulation 2.

Three-dimensional model simulations were carried out, where the molar flows in the system were presented as a function of the reaction time and the reactor length (volume) starting from the flow from the ejector to the upper part of the reaction vessel and ending at the flow from the loop into the ejector.

In the first simulation (Fig. 5), the correlation Eq. (6) with an α-value of 6.61×10^{-2} was used to describe the mass transfer in the ejector. The hydrogen mass-transfer rate in the reaction vessel was considered to be zero. The loop was considered as a cascade of 10 CSTRs.

As can be seen from the figure, the concentration of hydrogen becomes very low in the reactor as well as in the loop. Therefore almost all reactions take place in the upper part of the reaction vessel and the profiles in the direction of the reactor length become flat.

In Fig. 6, the hydrogen mass tranfer in the ejector was assumed to proceed instantaneously. The simulation indicates that there is hydrogen left at the outlet of the loop and especially hydrogen profile becomes very sharp. In this simulation, the loop was described with the axial dispersion model, the Peclet number being 2.56, which according to Salmi and Lindfors [11] corresponds to two tanks-in-series.

The third simulation (Fig. 7) was carried out by lowering the circulation velocity of the liquid from 1 to 0.05 m^3/min and the aldehyde feed rate was doubled. In this way, we obtained sharper profiles in both directions: in the direction of time and reactor

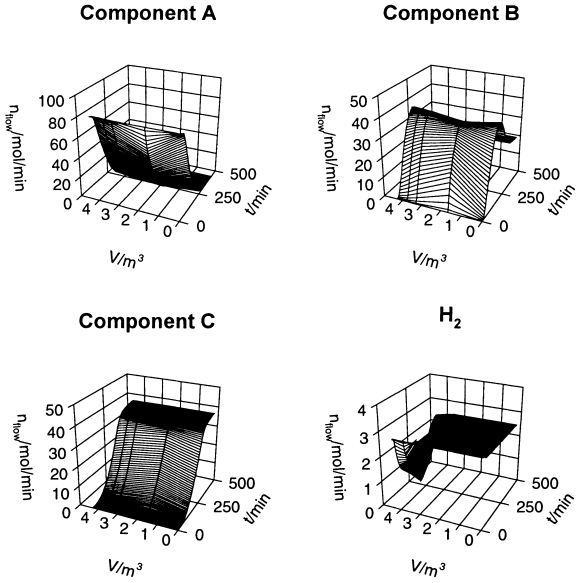

Fig. 7. Profile simulation 3.

length. The hydrogen mass-transfer resistance was assumed to be negligible both in the ejector and the reaction vessel. The reactions were shifted to proceed in the loop, which in this case was considered as two tanks-in-series.

9. Conclusions

The simulations above proved that the program package is able to simulate the reactions in the loop reactor under different conditions, and both CSTR and axial dispersion models are applicable. The reactor model was also verified to indicate the governing trends of reductive alkylation. Therefore, the simulation program is a useful tool for simulation of large-scale production in loop reactors.

10. Nomenclature

A	mass-transfer area (m^2)
a	specific mass-transfer area (m^2/m^3)
c	concentration (mol/m^3)
D	diffusion coefficient, axial dispersion coefficient (m^2/min)
G	volumetric gas flow in the ejector (m^3/min)
K	adsorption equilibrium coefficient
k	mass-transfer coefficient (m/min)
k	rate constant
L	volumetric liquid flow in the ejector (m^3/min)
l	length (m)
m	mass (kg)
N	flux (mol/m^2 min)
n	amount of substance (mol)
$\dot{n}$	molar flow (mol/min)
R	reaction rate
r	generation rate
t	time (min)
V	volume (m^3)
$\dot{V}$	volumetric flow (m^3/min)
w	velocity (m/s)
x	mole fraction

Greek letters

α	experimental coefficient Eq. (6)
ρ_B	catalyst bulk density (kg/m^3)

Subscripts

cat	catalytic, catalyst
ej	ejector
I	component index
k	reactor index
L	liquid phase
M	active metal
n	nozzle
noncat	non-catalytic
0	feed

Superscripts

s	saturation
$'$	reaction vessel
$''$	loop
$'''$	ejector

Acknowledgements

The project was financially supported by the Technology Development Centre (TEKES).

References

[1] C.W. Gear, Numerical Initial Value Problems in Ordinary Differential Equations, Prentice-Hall, Englewood Cliffs, NJ, 1971.
[2] W.E. Schiesser, The Numerical Method of Lines, Integration of Partial Differential Equations, Academic Press, San Diego, 1991.
[3] H. Haario, MODEST-User's Guide, Profmath Oy, Helsinki, 1994.
[4] C.A.M.C. Dirix, K. van der Wiele, Mass transfer in jet loop reactors, Chem. Eng. Sci. 45 (1990) 2333–2340.
[5] C.R. Wilke, P. Chang, AIChE J. 1 (1955) 265.
[6] P.G.T. Fogg, W. Gerrard, Solubility of Gases in Liquids, Wiley, Chichester, 1991, pp. 300–303.
[7] S. Ege, Organic Chemistry, Structure and Reactivity, 3rd ed., D.C.Heath and Comp., Lexington, 1994, p. 535.
[8] M.A. Fox, J.K. Whitesell, Organic Chemistry, Jones and Bartlett Publishers, Boston, 1994, p. 72.
[9] J.A. Nelder, R. Mead, A Simplex method for function minimization, Comput. J. 7 (1965) 308–313.
[10] D.W. Marquardt, An algorithm for least squares estimation on nonlinear parameters, SIAM J. (1963) 431–441.
[11] T. Salmi, L.-E. Lindfors, A program package for simulation of coupled chemical reactions in flow reactors, Comput. Indus. Eng. 10 (1986) 44–68.